Energy and Power Engineering, 2022, 14, 404-419
https://www.scirp.org/journal/epe
ISSN Online: 1947-3818
ISSN Print: 1949-243X

Modeling of the Coupling of the Lightning Shock Wave Flow Circuit in the High Voltage Electrical Network

Mwanamputu Mbwanzo[1], Timothée Nsongo[2], Pasi Bengi Masata Andre[3], Flory Lidinga Mobonda[4], Mathurin Gogom[5]

[1]Laboratory of Electrical Engineering, Higher Institute of Applied Technique DC, Kinshasa, The Democratic Republic of the Congo
[2]Laboratory of Physics, Marien Ngouabi University at the Science and Technology Facility, Brazzaville, Republic of Congo
[3]Laboratory of Electronics and Telecommunications, Higher Institute of Applied Techniques, DC, Kinshasa, The Democratic Republic of the Congo
[4]Laboratory of Electrical Engineering, Higher Institute of Applied Technique DC, Boma, The Democratic Republic of the Congo
[5]Laboratory of Electrical and Electronic Engineering, Marien Ngouabi University, Brazzaville, Republic of Congo
Email: clmwanamputu@gmail.com

How to cite this paper: Mbwanzo, M., Nsongo, T., Andre, P.B.M., Mobonda, F.L. and Gogom, M. (2022) Modeling of the Coupling of the Lightning Shock Wave Flow Circuit in the High Voltage Electrical Network. *Energy and Power Engineering*, **14**, 404-419.
https://doi.org/10.4236/epe.2022.148021

Received: May 28, 2022
Accepted: August 23, 2022
Published: August 26, 2022

Abstract

This article focuses on the aggression of lightning overload on the equipment of the electrical network of sites where storm activity is very dense; and the electrocution of people located in the direct environment of the high-voltage substation during the flow of lightning current to the ground through the ground socket. The modeling of the flow circuit of the shock wave consisting of guard wire, lightning arrester and ground socket couple to the transformer of the high voltage substations, thanks to the approach of a servo block, led to the synthesis of a PID regulator (corrector) whose action is to reject the effects of the overvoltage on the network equipment and to significantly reduce or even cancel the effects of the step or touch voltage due to the distribution of the potential around the ground socket; and thus improve the quality of service of the high-voltage transmission and distribution electricity network, especially in stormy times.

Keywords

Modeling, Coupling, Flow Circuit, Shock Wave, Lightning, Electrical Network, High Voltage

1. Introduction

The flow of the shock wave of lightning or a fault current into any electrical sys-

tem is ensured by the grounding of all metal parts of the latter (substations and high voltage lines) through a path of low impedance in order to ensure the protection of people and property and this in accordance with standards [1] [2].

When injecting the lightning current into the ground, the characteristic parameter that makes it possible to evaluate the response of the ground intake is its transient impedance which is a function of the injected current and the characteristics of the soil.

While approaches to modeling power grid components for their protection against short-circuit current and other defects at industrial frequency have been obtained by analytical and experimental methods, modeling the flow circuit of high-frequency pulse type lightning current [3] [4] [5] in a resistivity soil that varies according to the season and its nature has always been complex.

In most publications, the use of the finite element or finite difference method has been discussed for the study of the spaco-temporal distribution of the electric field in order to evaluate the transient response of the grounding system.

Recent studies on the performance of grounding systems in high-voltage substations [6] [7] analyze the impact of the integration of materials of low LRM resistivity in the realization of grounding grids as well as the factors affecting the grounding impedance and the characteristics of the large grounding grid with a view to providing a technical reference for the design, the operation and maintenance of a large grounding network.

This publication, on the other hand, uses the servo system approach, where the transient impedance is obtained by modeling all the impedances of the network protection elements, from the point of impact to the ground network of the system.

This approach made it possible to synthesize a regulator (corrector) capable of rejecting the effects of lightning current before it reaches the equipment and increases the potential of the ground intake that can cause electrocution of people and animals in the direct environment of the substation or high voltage line.

2. Modeling of the Flow Circuit of the Shock Wave of the HT Substation

2.1. Lightning Current Model

Theory shows and experience confirms that the shape of the lightning discharge current is bi-exponential [8] and its temporal evolution is represented by the curve in **Figure 1** below:

$$I(t) = I_0\left[\exp(-\alpha t) - \exp(-\beta t)\right] \tag{1}$$

The numerical values of the lightning parameters α et β of the bi-exponential equation [3] made it possible to obtain the pace of the curve of the figure below confirmed in theory and experimentally.

The lightning surge in electrical grid equipment results in sudden variation $\frac{\mathrm{d}i}{\mathrm{d}t}$ in lightning current on the transmission line.

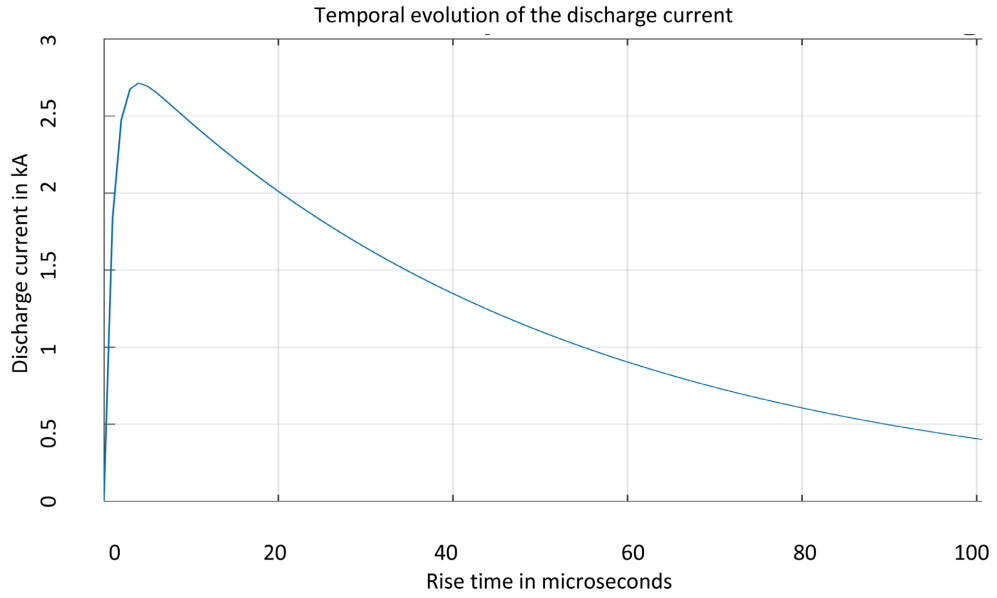

Figure 1. Lightning current speed.

$$u = Ri(t) + L\frac{\mathrm{d}i(t)}{\mathrm{d}t} \tag{2}$$

By comparing the equation below to the induced electromotive force, the current lightning model in the Laplace domain becomes;

$$I(s) = \frac{\mu I_0 S}{2\pi r L}\left[\frac{\beta(s+\alpha)-\alpha(s+\beta)}{(s+\alpha)(s+\beta)\left(s+\frac{R}{L}\right)}\right] \tag{3}$$

The temporal lightning current flowing to the ground through the earth electrode represented by **Figure 1** reaches its peak for values greater than 2.5 × 10 kA in a few microseconds.

Following Frédéric ELIE's publication "*Lightning* and pitch voltage November *2005*", *the parameters of the lightning current are determined experimentally and have the following values:*

α = 0.02 µs, β = 1 µs, for a current amplitude of I_0 = 30 kA. µs β µs

The rise time to reach the peak of the wave is obtained by:

$$t_m = 1/(-\alpha)\cdot\ln(\beta/\alpha) \tag{4}$$

The order of magnitude is t_m = 2.2 s.µ

The peak of the bi-exponential lightning current shown in **Figure 2** constitutes shock energy; therefore, aggression to the equipment of the electrical network and presents a danger for people located in an environment close to the station.

2.2. Watching Model

The guard wire located at the top of transmission line pylons shown in **Figure 2**

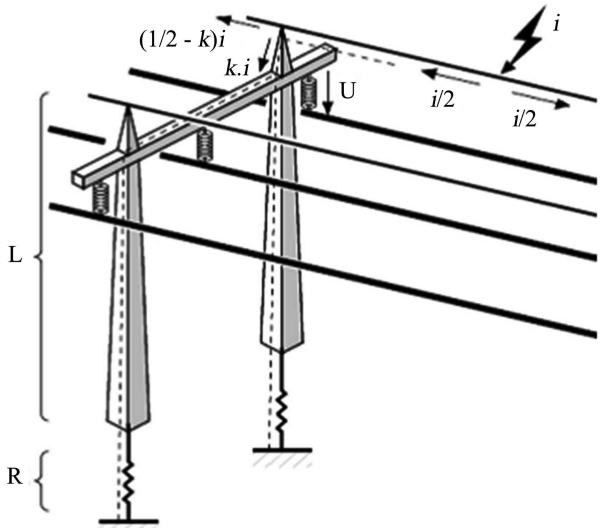

Figure 2. Frédéric Élie, November 2005, http://fred.elie.free.fr/.

also plays the role of lightning current detection; it is also used for the transmission of the high frequency signal of telecommunication between the production centers and the distribution networks in the consumption centers.

This ground wire is connected to the ground via an L-inductor cable through the pylon and a very low-value R-series resistor.

The guard wire surge transfer function translated by Equation (2) gives:

$$F_1(s) = \frac{I(s)}{U(s)} = \frac{1}{R + Ls} \tag{5}$$

$F_1(s)$ is the transfer function of the line guard cable and the numerical values of the numerical values of $R = 0.07\ \Omega$ and $L = 1.01\ m_H$ are given in the table of characteristics of the line 220 kV. These values come from the National Electricity Company, SNEL/RDC [9].

$$F_1(s) = \frac{1}{0.07 + s} \tag{6}$$

2.3. Model of the Transformer of the HV Substation in Overvoltage [10]

For the study of the phenomenon of overvoltage transmitted to the transformer of the HV substation by coupling with the flow circuit, one limits oneself to an equivalent diagram of a winding on the high voltage side in **Figure 3** below.

This equivalent diagram reflects the initial distribution of the overvoltage that propagates in the power transformer of the substation.

The application of the Kirchhoff equation to node P in **Figure 3** gives.

$$i + i_k - \left(i - \frac{\partial i}{\partial x}dx\right) - \left(i_k + \frac{\partial i}{\partial x}dx\right) - i_c = 0 \tag{7}$$

$$i_c = -\frac{\partial(i + i_k)}{\partial x}dx \text{ and } i_c = -c\frac{\partial u}{\partial t}dx \tag{8}$$

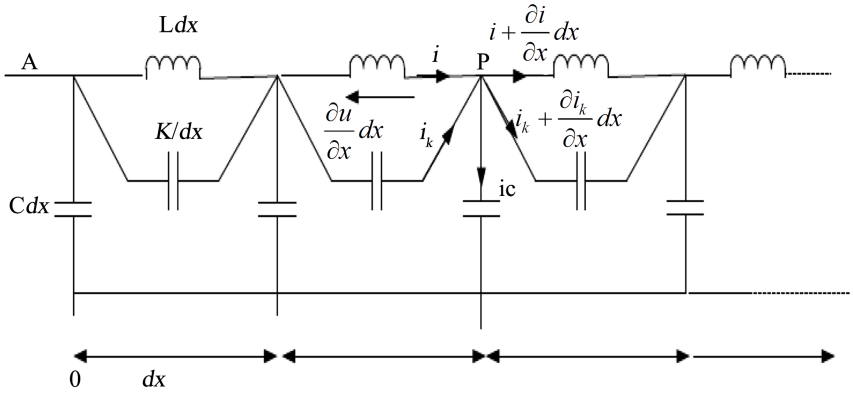

Figure 3. Equivalent diagram of a surge transformer phase.

Expressions of Equation (8) gives

$$\frac{\partial\left(i+i_k\right)}{\partial x}=-c\frac{\partial u}{\partial t}\rightarrow i_k=-\frac{k}{dx}\frac{\partial^2 u}{\partial x\partial t}dx\rightarrow\frac{\partial i_k}{\partial x}=-c\frac{\partial^3 u}{\partial x^2\partial t} \tag{9}$$

The current in inductor of equivalent diagram

$$\frac{\partial i}{\partial t}=-\frac{1}{L}\frac{\partial u}{\partial x}\rightarrow\frac{\partial u}{\partial x}=-L\frac{\partial i}{\partial t} \tag{10}$$

$$\frac{\partial\left(i+i_k\right)}{\partial x}=-\frac{1}{L}\frac{\partial u\partial t}{\partial x^2}-c\frac{\partial^3 u}{\partial x^2\partial t} \tag{11}$$

Ask $i+i_k=i_a$ and $\frac{\partial X}{\partial t}$ being the propagation speed of the overvoltage in the transformer V,

We have:

$$\frac{\partial i_a}{\partial t}=-\frac{1}{V}\left[\frac{1}{L}\frac{\partial u}{\partial t}+C\frac{\partial^3 u}{\partial t^3}\right]\rightarrow V=-\frac{1}{L}\frac{\partial u}{\partial t}-C\frac{\partial^3 u}{\partial t^3} \tag{12}$$

V is the speed of the surge wave in the tr with almost low attenuation ($V=3\times10^8$ m·s^{-2}),

In frequency mode, the Equation (12) becomes:

$$F_2(s)=\frac{U(s)}{I(s)}=\frac{-V}{\frac{1}{L}+CS^2} \tag{13}$$

The numerical values of $F_2(s)$ are given *Ru, pu = 0.01 pu*; *Xu,pu = 0.04 to 0.18*; X_L *= 0.1 to 0.2* [9].

The transformer transfer function during the overvoltage becomes:

$$F_2(s)=\frac{U(s)}{I(s)}=\frac{-V}{\frac{1}{0.2}+0.04S^2} \tag{14}$$

2.4. Model of the Nonlinear Resistance of the Elements of the Zinc Oxide Lightning Arrester (ZnO)

The behavior of the non-linear resistance of the variance elements ZnO is

represented by a current expression as a function of voltage ($V = F(I)$), extracted in the voltage-current characteristic of the lightning arrester.

The non-linear behavior of the ZnO elements of the lightning arrester is mainly due to non-linear resistors and capacitors as represented by the figure below.

Equation (23) below reflects this nonlinearity [11].

$$I = K_1 V^{\alpha_1} + K_2 V^{\alpha_2} \tag{15}$$

where:

I: Current in mA;

V: Voltage in kV;

α: Coefficient of non-linearity of lightning arrester varistors: $30 < \alpha < 100$;

K: Dielectric constant of materials specific to the lightning arrester: $K_1 = K_2 = 100$.

By generalizing, we obtain:

$$I = KV^{\alpha} \tag{16}$$

Since the numerical values of and K are very large, we can linearize this expression by the characteristic of the lightning arrester below in the area between U_p and U_c respectively: priming voltage (protection level) and lightning arrester set voltage (maximum permanent working voltage).

In this linear area between U_c and U_p of **Figure 4**, the character takes the form: $y = ax$

$$I = KV \tag{17}$$

where:

$K = \dfrac{U_P - U_C}{I_c - I_n}$ being the slope of the line et V a potential difference seen the characteristic in its part U_C and U_P, we can then write:

$$i(t) = K\frac{\mathrm{d}v}{\mathrm{d}t} \tag{18}$$

In the field of Laplace, we get

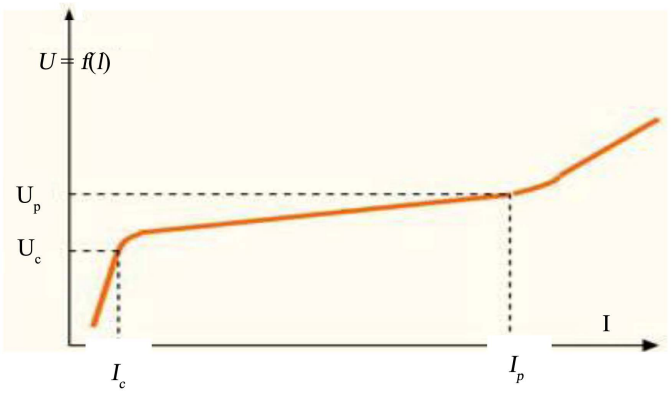

Figure 4. characteristic $U = f(i)$ of the varistor. Where: U_p: level of protection against lightning strike; U_c: steady-state voltage.

$$F_3(s) = \frac{I(s)}{U(s)} = \frac{K}{s} \tag{19}$$

$F_3(s)$ is the transfer function of the zinc oxide surge arrester used in the HT substation.

Les values of U_c = 225 kV, U_p = 245 kV, I_c = 100 kA and I_n = 20 kA according to the manufacturers [11].

The coefficient K becomes:

$$K = \frac{U_p - U_c}{I_c - I_n} = \frac{245 - 225}{100 - 20} = 0.25$$

In the field of Laplace, subject to the hypotheses mentioned above, we have:

$$F_3(s) = \frac{I(s)}{U(s)} = \frac{0.25}{s} \tag{20}$$

$F_3(s)$ is the model of the lightning arrester.

2.5. Model of the Land Network of the HV Substation

In an electrical energy transmission network with HV lines and substations, grounding is carried out in several forms [12] [13]:

- Simple grounding systems, simple electrodes;
- Complex grounding systems, such as the large ground grids of the HT substation illustrated in **Figure 5**.

From the above, the grounding grid of the substation is assimilated to a transmission line characterized by an input quantity (the lightning current) and an output quantity (the potential difference around the ground socket).

Modeling of the propagation of the lightning current through the grounding grid must therefore use a description of the transmission line by constants distributed by the following expressions:

$$\frac{\partial i}{\partial t} = Gu(x,t) + C\frac{\partial u}{\partial t} \tag{21}$$

$$\frac{\partial u}{\partial t} = Ri(x,t) + L\frac{\partial i}{\partial t} \tag{22}$$

Equations (21) and (22) are called telegraph equations translating the variation in time and space of current and voltage along the overvoltage line.

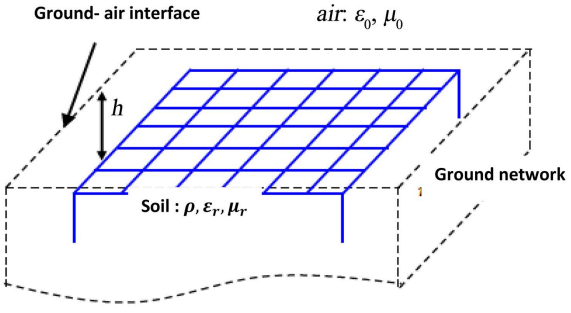

Figure 5. HV station grounding grid (Daoud SEKKI, 2016).

Hypothesis:

The ground network of HV substations being local and of small dimensions, we can admit that the flow of current in the ground is mainly through the transverse elements; the current and the distribution of the potential around the ground socket are weakly related to the variable *x*.

Thus: only Equation (23) and the time variable are taken into account. The expression (21) becomes:

$$\frac{\partial i}{\partial t} = Gu(t) + C\frac{\partial u}{\partial t}$$

Laplace's transform gives:

$$F_4(s) = \frac{U(s)}{I(s)} = \frac{s}{G + Cs} \tag{23}$$

$F_4(s)$ is the transfer function of the grounding grid of the HT station.

G and C shave the transverse parameters of the interconnected network (underground grounding grid) whose numerical values are obtained by the following assumptions:

- ✓ The soil is homogeneous and its characteristic parameters are constants; ε, μ et ρ.
- ✓ The reinforcements of the capacitor thus formed are the different layers of the ground and the grounding grid.

In the realization of the ground network of HT substations, some standard values are recommended by the standards (NFC 13 - 100 and NFC 11 - 200, CEI 61140, IEEE 80 - 2000) [14]:

- Dimensions of the grounding grid, GTC-25/4 series are: 2.50 × 0.4 m;
- Soil characteristics [8]: m; $h \le 1\,\text{m}$; $\varepsilon_r = 5$; $\mu_r = 1$ et $\rho = 10\,\Omega\cdot\text{m}$.

These parameters make it possible to define the permittivity and relative permeability (ε_r, μ_r) in relation to their values in a vacuum [15] [16]:

- $\varepsilon_r = \frac{\varepsilon}{\varepsilon_0}$ is the relative permittivity and is $\mu_r = \frac{\mu}{\mu_0}$ the relative magnetic permeability,

ε_r and μ_r are the corresponding permittivity and permeability of the soil.

In the majority of cases, we $\mu = \mu_0$ consider; for $\mu_r = 1$.

➢ For the resistance of the grounding of the station, we have:

$$R = \frac{\rho}{4r} \text{ and } r = \sqrt{\frac{ab}{\pi}} = \sqrt{\frac{2.50\times 0.4}{3.14}} = 0.56 \text{ and } R = \frac{10}{4\times 0.56} = \frac{10}{2.24} = 4.4\,\Omega$$

This value is acceptable by the standard and gives rise to high grounding performance ($R < 10\,\Omega$); a and b are respectively the length and width of the grid.

The conductance G becomes: $G = \frac{1}{R} = \frac{1}{3.5} = 0.28\,\Omega^{-1}$

➢ For the capacity of the ground circuit

$$C = \varepsilon\frac{S}{a} \text{ and } \varepsilon = \varepsilon_0\varepsilon_r = 5\times 8.85\times 10^{-12}\times 10^{-12}$$

S = surface of the reinforcements = 2.50 × 0.4 = 1 m^2

$$C = \varepsilon \frac{S}{a} = 44.25\ \text{F} = 11\ \text{pF} \times 10^{-12} \times \frac{1}{4} = 11 \times 10^{-12}$$

The numerical values of G and C of the transfer function of the terrestrial network being determined, we can write:

$$F_4(s) = \frac{s}{0.28 + 0.01s} \tag{24}$$

The nettle of the system: $V_{ps}(s)$ desired pitch voltage during the flow of lightning current on the ground.

After obtaining all the transfer functions of the components of the surge wave flow circuit of the HV substation coupled with the power transformer and, using the servo system approach, the functional block diagram of the circuit of Lightning shock wave flow is given in Figure 6 below:

The transfer function $F(s)$ of the components of the direct cascade flow circuit becomes:

$$F(s) = F_1 F_3 F_4 \tag{25}$$

$F(s)$ represents the transient impedance of the circuit which must act on the flow velocity of the lightning current on the ground; this lightning current is considered a disturbance to the system. Below is the pace of the index response of $F(s)$ under the action of the disturbance.

The observation in Figure 7 below, the curve shows that the corrected system is stable. Nevertheless, it has a static error of the order of 7%, the system is therefore imprecise; it is, therefore, necessary to correct it so that the output is the image of the input regardless of the presence of the disturbance.

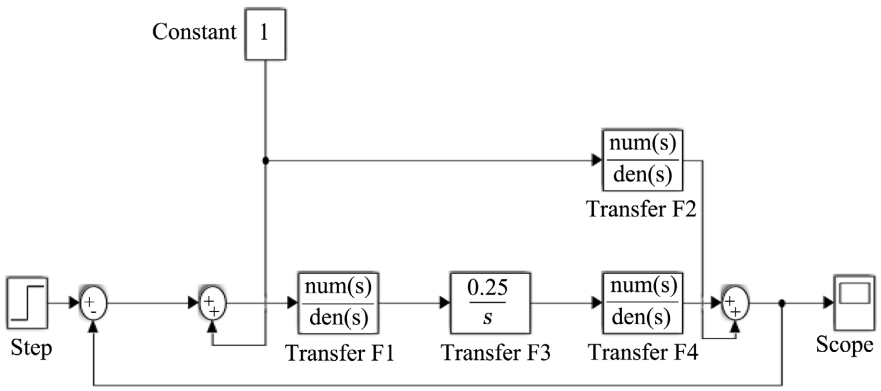

Figure 6. Functional block of the ground shock wave flow. Circuit. Legend:

$$F_1 = \frac{num(s)}{den(s)} = \frac{numerator(s)}{denominator(s)} = \frac{1}{0.07 + s};$$

$$F_2 = \frac{num(s)}{den(s)} = \frac{numerator(s)}{denominator(s)} = \frac{-V}{\frac{1}{0.2} + 0.04s^2}; \quad F_3 = \frac{num(s)}{den(s)} = \frac{numerator(s)}{denominator(s)} = \frac{0.25}{s};$$

$$F_4 = \frac{num(s)}{den(s)} = \frac{numerator(s)}{denominator(s)} = \frac{s}{0.28 + 0.01s}.$$

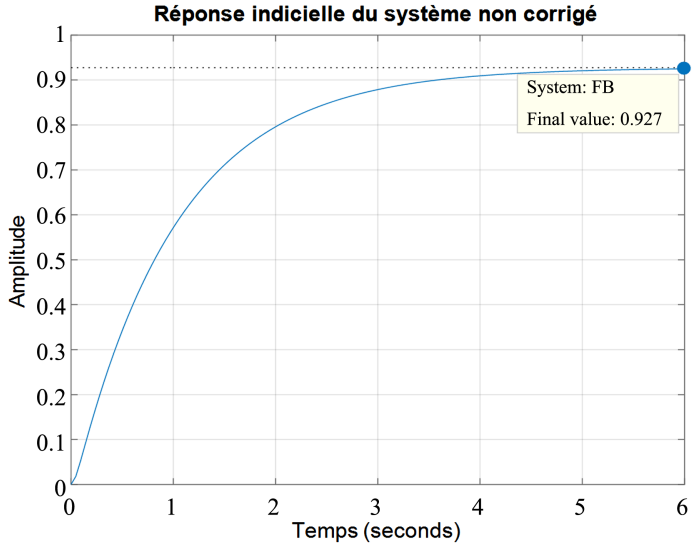

Figure 7. System index response not corrected.

Considering that the aggressiveness of lightning can have an impact directly on the flow circuit and the transformer of the substation, the block diagram of the closed-loop circuit with unit return gives them to the block diagram below in **Figure 8**.

The output of the closed-loop system taking into account the disturbance and the overvoltage induced in the transformer makes it possible to write:

$$S(B)=\frac{C(s)F(s)}{1+C(s)F(s)}+\frac{F(s)}{1+C(s)F(s)}+\frac{F_2(s)P(s)}{1+C(s)F(s)} \tag{26}$$

Faced with the imprecision presented by $F(s)$, it is essential to synthesize a corrector whose role is to reject the disturbance $P(s)$.

Summary of the corrector $C(s)$

A closed-loop, $F(s)$ although of the second order, has two transmittances of the first order cascading with a dominant pole of the form:

$$F(s)\cong\frac{0.25}{(s+1)(s+27.1)} \tag{27}$$

Experience and theory support that the response time for a first-order system is $t_r=3\tau$ since, $\tau=1\,\text{s}$ then

$$\frac{Tr_{5\%}}{T_m}=\frac{3\tau}{2.2}=\frac{3}{2.2}=1.36 \quad \text{et} \quad t_r=1.36\times 2.2\cong 3\,\mu\text{s}$$

The transfer function of the PID regulator has the form:

$$C(s)=P+\frac{I}{s}+D\frac{N}{1+\frac{N}{s}} \tag{28}$$

Thanks to the digital tool Matlab, Simulink, the toolbox "PID turner" below, we can determine the parameters of the correct **Figure 9**: Modeling of the flow circuit of the shock wave environment Matlab Simulink.

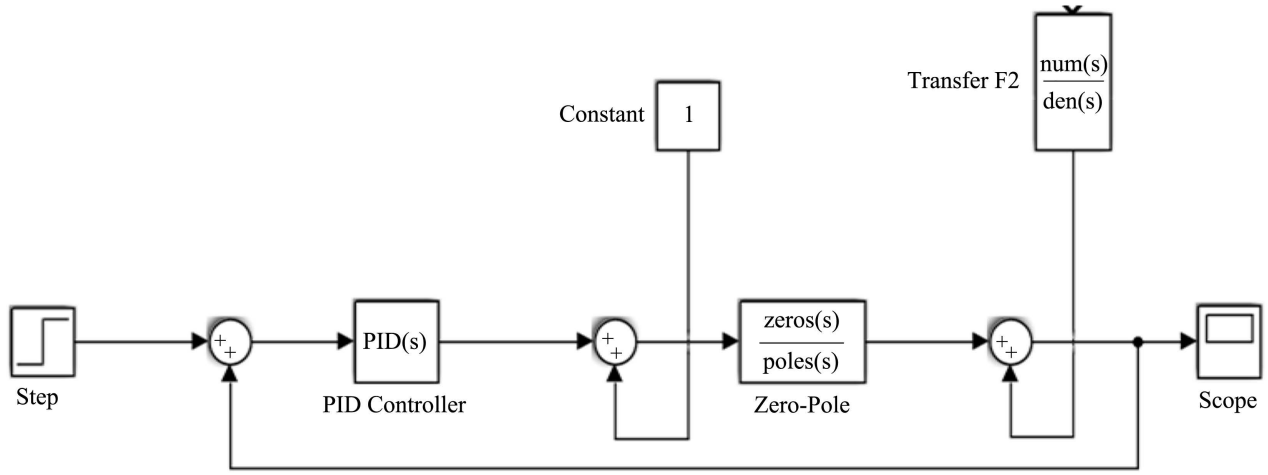

Figure 8. Block diagram of the flow circuit with insertion of the corrector under Matlab Simulink. Legend: PID: Proportional, integral, differentiator.

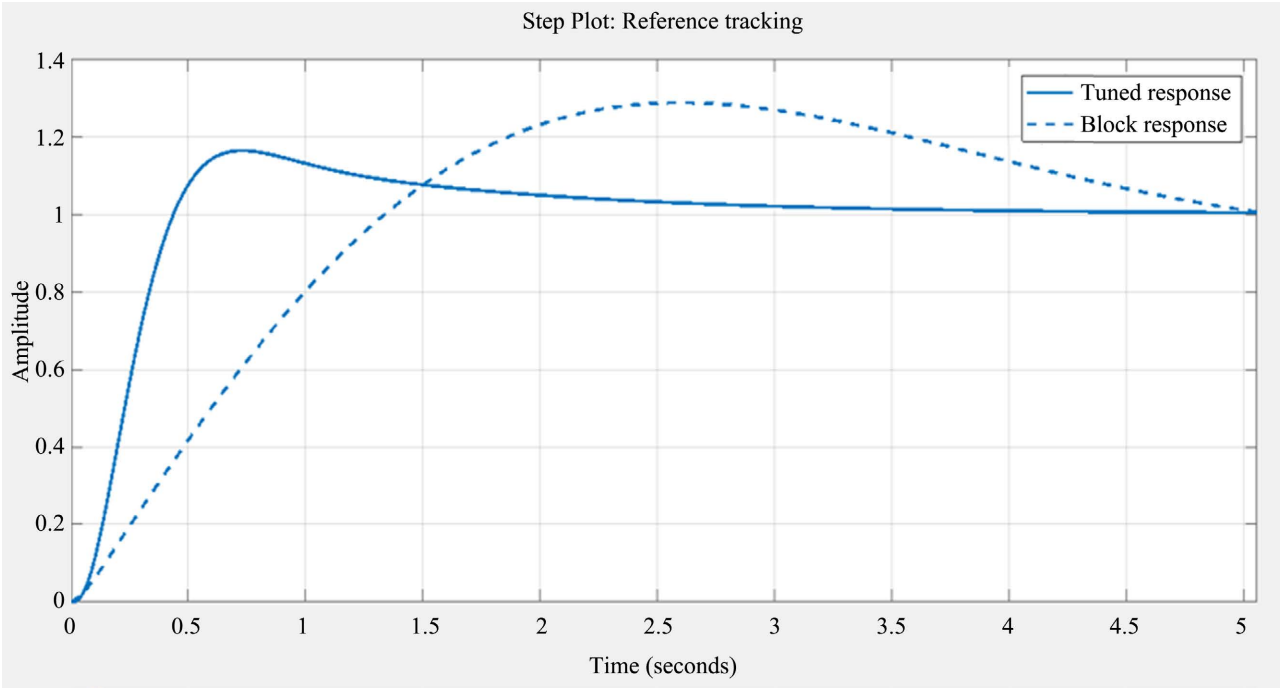

Figure 9. System response before dotted curve correction and after continuous correction.

The simulation results are recorded in **Table 1**.

The corrector settings are: $P = 4.3347$; $I = 3.303$; $D = -0.30048$; $N = 14.4257$.

N is softening pole, which means, a correction pole.

$$C(s) = \frac{U(s)}{\varepsilon(s)} = 4.3347 + \frac{3.3103}{s} - \frac{-0.030048 \times 14.4257}{1 + \frac{14.4257}{s}}$$

$$C(s) = \frac{U(s)}{\varepsilon(s)} = 4.3347 + \frac{3.3103}{s} - \frac{-4.3346s}{s + 14.4257} = \frac{-62.2s}{s^2 + 14.43s}$$

Table 1. Recording system simulation results.

controller parameters	
P	4.3347
I	3.3103
D	−0.30048
N	12.4257
Performance and Robustness	
	Tuned
Rise time	0.283 seconds
Settling time	3 seconds
Overshoot	16.30%
Peak	1.16
Gain margin	19.4 Db@ 19.4 rad/s
Phase margin	57.2 der @ 3.96 rad/s
Closed-loop stability	Stable

$$C(s)=\frac{U(s)}{\varepsilon(s)}=\frac{-62.2}{s+14.43} \tag{29}$$

The expression (34) represents the transfer function of the corrector sought.

The simulation consists in determining the parameters of the digital PID regulator that will have to meet certain specifications of the optimal specifications according to the standard which should be exceeded; 20% gain margin of 6 to 20 dB and phase margin between 45˚ to 65˚; these two parameters reflect the robustness of the system.

The effects of the correction after simulation are given by the following curves:

The look of the curves in Figure 9, obtained from Simulink's PID Turner subprogram, shows that the system response meets the requirements of the specifications.

Dotted, uncorrected system response and continuous, corrected system response that shows stability in a very short time after reaching its peak.

Thanks again to the program PID Turner, it can be seen that the rejection of the disturbance by the corrector is the reverse corrected response

If the curves in Figure 10(a) and Figure 10(b) reflect the response of the system in time, the figures below reflect the same response of the system in frequency regime under the action of the corrector.

The effect of the rejection of the lightning current is also observed in Figure 11, this time in the frequency domain, translated by the Bode curve according to the phase margin and the gain margin by the specifications defined below.

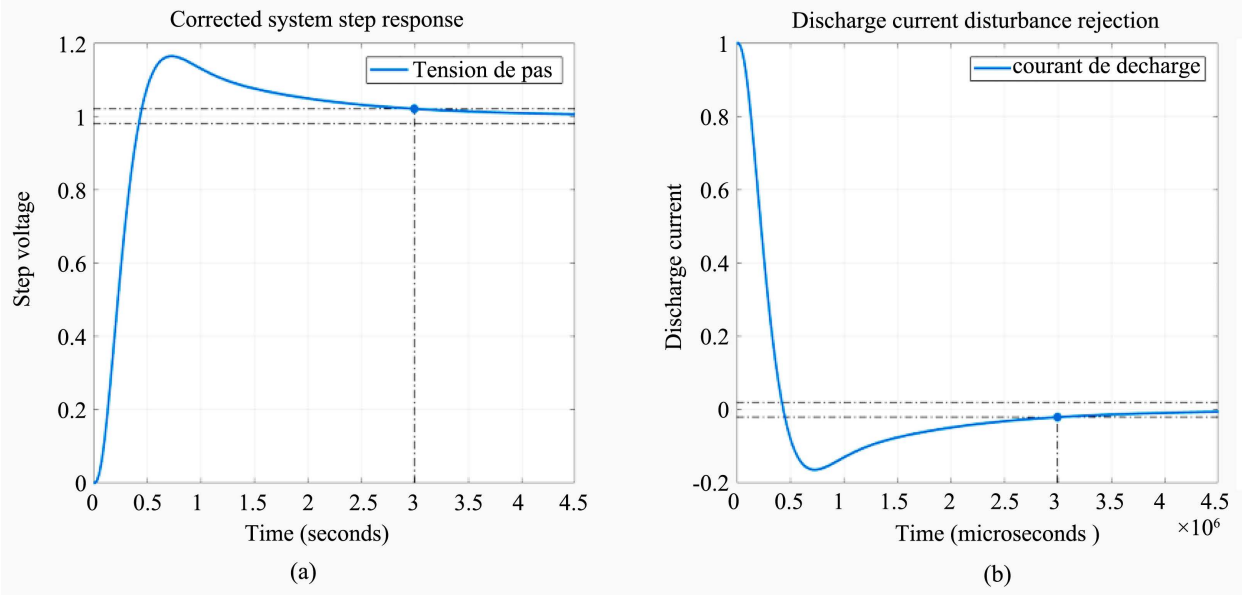

Figure 10. (a) and (b): Corrected response and rejection of disturbance.

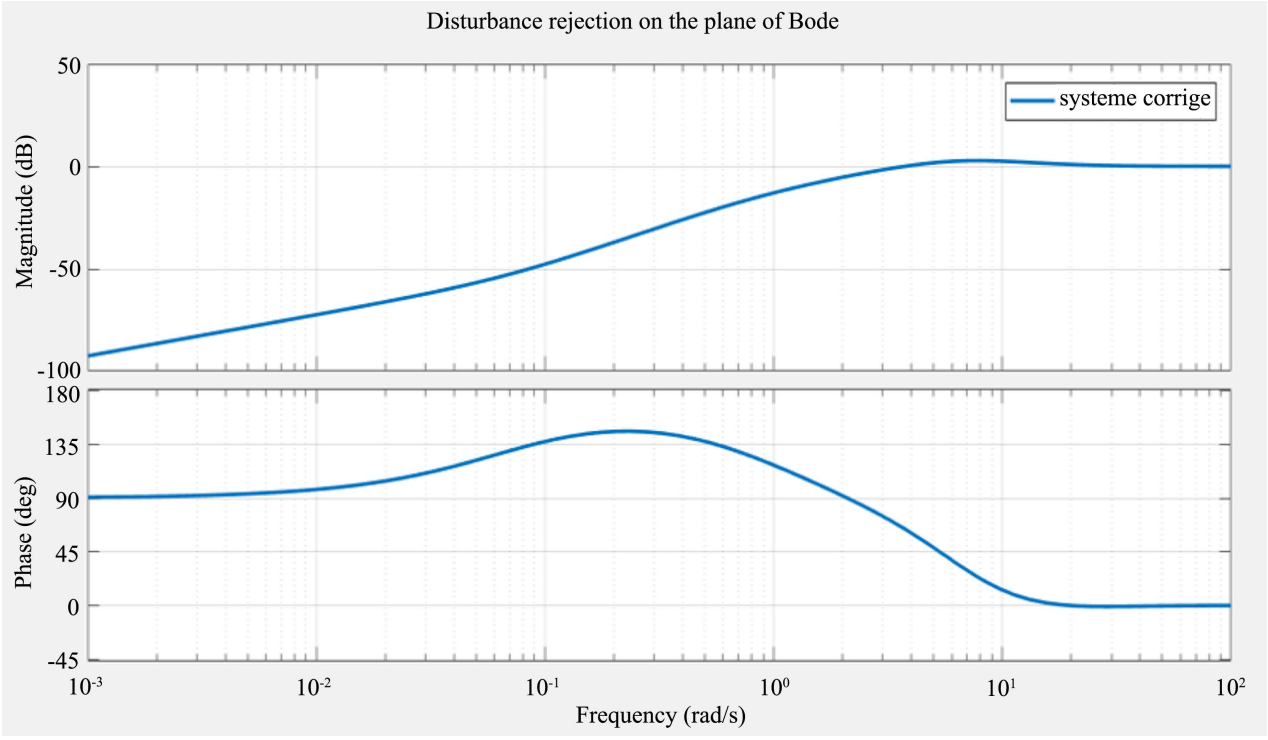

Figure 11. Response of the flow circuit on the plane of bode.

The effect of the rejection of the lightning current is also observed in Figure 11, this time in the frequency domain, translated by the Bode curve according to the phase margin and the gain margin by the specifications defined above.

3. Discussion

In the research work of Djamel IDIR [17] on Modeling and Simulation of an

Atmospheric Discharge on Earthing Grids, he showed the influence of temporal changes in the protective characteristics against atmospheric discharges.

KEVIN APOTE A. TETE [18], on the other hand, in his research, focused on the Transient Response of Lightning Strikes on Wind Installations, has to evaluate the frequency and temporal responses in the grounding systems of wind turbines disturbed by lightning.

A.SELLIER and his Companions [19] [20], in their work, focused on the impact of the soil on the impedance of an earth intake by the experimental and numerical approach, compared two soil models with horizontal layers with different resistivity's the value of the impedance of an earth intake subjected to a lightning-type pulse.

The results of this research have led to show the influence of soil characteristics on the transient response of the grounding grid system and the contribution of the impedance value of an earth intake in the dimensioning of lightning protection systems,

and also the importance of choosing the injection point of the lightning current in order to reduce the peak of the potential by approaching the center of the grid in order to significantly reduce the risk of electrocution.

Our work on the aggression of lightning surge on electrical network equipment has taken into account all the components of the ground lightning flow circuit (from the guard cable, lightning arrester, and grounding grid) to the power transformer in order to obtain the model of the transient impedance of the flow circuit.

From this model, the PID regulator model was synthesized with the aim of rejecting the effects of lightning overload on electrical network equipment.

Our point of convergence with the work mentioned above is focused on transient impedance and soil characteristics in order to size the lightning protection device.

F. Elie in his publication on "Lightning and pitch voltage November 2005" [9], showed that the rise time of 2 μs is sufficient for the intensity of the lightning current to reach its peak by introducing the propagation parameters α and β of the Equation (1).

In this article, we obtained the response time of 3 μs for the corrector to reject the lightning disturbance; it can therefore be said that the flow circuit with the integration of the regulator meets the criterion of speed required for stability.

4. Conclusions

This publication consisted of the synthesis of a corrector (regulator) capable of rejecting or even dampening the effects of lightning shock energy on the power equipment of the high-voltage electrical network and significantly reducing the cases of electrocution due to the distribution of the potential around the ground socket.

The functional block approach of a servo system used made it possible to obtain an open-loop index response of the transient impedance of the ground

lightning current flow circuit coupled to the power transformer with an error of 7%; which effectively shows that the increase in potential during the flow of lightning on the ground leads to an aggressive overvoltage on the equipment and electrocution in an environment close to the ground socket.

The parameters of the PID regulator obtained and the response time of 3 μs of the flow circuit to the lightning disturbance give rise to the precision and stability of the circuit supported by the different curves obtained after simulation thanks to the digital tool Matlab Simulink and this in accordance with the specifications imposed by the characteristics of the impedance of the flow circuit without integration of the regulator and the stability criteria of automatic regulation.

These results are encouraging because they meet the requirements of the International Electrotechnical Commission in its IEC 62305-01 standard for lightning protection equipment for high-voltage electrical installations.

Conflicts of Interest

The authors declare no conflicts of interest regarding the publication of this paper.

References

[1] NFC 13 100 (2015) Delivery Stations Powered by a Public HTA Distribution Network (Up to 33 kV).

[2] NFC 13 200 (2009) High Voltage Electrical Installations—Additional Rules for Production Sites and Industrial, Tertiary and Agricultural Installations.

[3] IEC 62305-1 (2010) Protection against Lightning—Part 1: General Principles.

[4] IEC 62305-3 (2010) Protection against Lightning—Part 3: Physical Damage to Structures and Life Hazard IEC.

[5] Ait-Amar Djennad, S. (2015) Lightning Protection, General Principles and Standards, Engineering Technique.

[6] He, J.L. and Zeng, H. (2006) Lightning Impulse Performances of Grounding Devices Covered with Low Resistivity Materials. *IEEE Transactions on Power Delivery*, **21**, 1706-1713.

[7] Li, Z.Z., Wang, S., Guo, F. and Zhang, B. (2017) Study Characteristics of Grounding Impedance of Large Grid. 2017 *IEEE International Conference on Environment and Electrical Engineering and* 2017 *IEEE Industrial and Commercial Power Systems Europe* (*EEEIC/I&CPS Europe*), Milan, 6-9 June 2017, 1-4.

[8] Frédéric Elie, "Lightning and step tension", November 2005

[9] Elie, F. (2004) Electrical Safety.

[10] Lilien, J.-L. (1999/2000) Transmission and Distribution of Electrical Energy, Manual of Practical Work for the Course. University of Liège, Liège.

[11] Mechati, M. (2010) Modelling of the ZnO Varistance Lightning Arrester for the Study of the Improvement of Its Electrical Properties. Magister Thesis, University of Badji Mokhtar, Annaba.

[12] ABB AB (2009) High Voltage Products: Lightning Arrester.

[13] Rouibah, T. (2015) Contribution to the Modeling and Simulation of Earth Intakes

of Electrical Installations. PhD Thesis, Ferhat Abbas University, Sétif.

[14] Sekki, D. (2016) Complex Topolgy Grounding Modeling by Line Theory. Doctoral Thesis, Mohamed Seddik University, Algeria.

[15] Rajotte, Y. (2018) Network Grounding, Hydro Quebec.

[16] RTE (2018) Safety for Network Electricians.

[17] Recommendation ITU-R, Soil Characteristics, Series P: Propagation of Radioelectric Waves, Genesis, 2018.

[18] Idir, D. (2017) Modeling and Simulation of an Atmospheric Discharge on Earthening Grids. Université du Québec En Abitibi-Témiscamingue, Québec.

[19] Tete, K.A.A. (2019) Transitional Response of Lightning Strikes on Wind Installations. Université du Québec En Abitibi-Témiscamingue, Québec.

[20] Sellier, A., Grange, F., Journet, S., Kouassi, A. and Dawalibi, F. (2018) Impact of the Soil on the Transient Impedance of a Tertre Intake: Numerical and Experimental Approach. *EMC Symposium*, Paris, July 2018, 3-4.